Photo Voltaic System Based HERIC and H6 Transformerless Inverter Fed Induction Motor

B. MADHU KIRAN[1], K. RAVI KUMAR[2], A. KIRAN SAI[3], SD. ABBAS HUSSAIN[4], T. NAGA KRISHNA SAI[5],

[1]Associate Professor, Dept of EEE, PSCMRCET, AP, India, E-mail: mkbaba9@gmail.com.
[2]UG Scholar, Dept of EEE, PSCMRCET, AP, India, E-mail: ravi217219@gmail.com.
[3]UG Scholar, Dept of EEE, PSCMRCET, AP, India, E-mail: kiransai.arepalli@gmail.com.
[4]UG Scholar, Dept of EEE, PSCMRCET, AP, India, E-mail: syedabbashussain287@gmail.com.
[5]UG Scholar, Dept of EEE, PSCMRCET, AP, India, E-mail: tkrishnasai308@gmail.com

Abstract: The elimination of the transformer in solar photovoltaic inverters has reduced the size, the weight and the losses in the system. On the other hand, the galvanic connection between the DC source and the grid generates leakage current through the earth parasitic capacitance. The leakage current depends on both the inverter topology and the control strategy. Among the existing inverters is the Highly Efficient and Reliable Inverter Concept (HERIC) topology that has low leakage current level and high efficiency. However, this topology suffers from low frequency harmonics and current zero crossings distortions. To eliminate these harmonics and distortions, a new transformerless inverter is proposed. The proposed system can be implemented by induction motor and this helps in improving of IM phase current, thereby reducing the torque ripple .Finally a Matlab/Simulink based model is developed and simulation results are presented.

Key Words: **Common-mode voltage, grid-tied inverter, leakage current, photovoltaic (PV) generation system, transformerless inverter, Induction motor.**

I. INTRODUCTION

Nowadays, the invention and development of new energysources are increasing due to the poisonous results causedby oil, gas and nuclear fuels. This has led the renewableenergy sources especially the solar PV systems to the prime position in the generation of electricity [1-2]. Photovoltaic have applications ranging from small power supplies to power grids. Photovoltaic systems connected to the grid have several advantages such as simplicity in installation,high efficiency, reliability and flexibility [3]. With a reduction in system cost PV technology seems to be an efficient means of power generation. A solar grid connected power generating system usually consists of a solar panel in which the solar cells are arranged to track sunlight, an inverter to convert the DC to AC and the induction motor.

This paper evaluates a single phase transformerless inverter topology called H6, which can minimize the dangerous leakage currents between the solar power generation system and the electrical load. Transformers are employed in the grid tied systems to provide a galvanic isolation between the PV panel and the grid for safety considerations [4-6].Lin efrequency transformers were employed in most of the PVgrid tied inverters. But in line frequency transformers due to their low frequency, the size, cost, weight etc. will be higher. The next option is the high frequency transformers. The usage of high frequency transformers increases the number of power stages which affects the efficiency in an adverse manner [7-8]. When these transformers are eliminated there will be a galvanic connection between the solar rmodule and the grid which results in a potential fluctuation between the PV array and the ground [9].The potential variation leads to the flow of common mode leakage currents that has to be eliminated which otherwise leads to electromagnetic distortions, interferences, harmonics andother power quality issues. The H6 transformerless inverter topology with unipolar sinusoidal PWM strategy seems to be a better solution to reduce these leakage currents by maintaining the common mode voltage constant [10]. A The blockdiagram for the system is shown in fig 1.

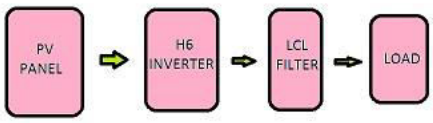

Fig.1 Block Diagram

However, the inverters with high-frequency transformers have several power stages, which increase the system complexity and reduce the system efficiency [1]–[6]. As a result, the transformerless PV grid-tied inverters, as shown in Fig.2, are widely installed in the low-power distributed PV generation systems.

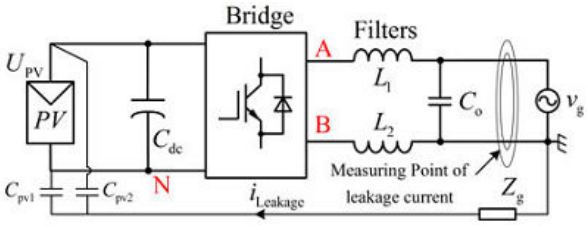

Fig.2. Leakage current path for transformerless PV inverters.

As shown in Fig.2, the leakage current Leakages flowing through the loop consisting of the parasitic capacitances(C_{PV1}andC_{PV2}), bridge, filters(L_1andL_2), utility grid, and ground impedanceZ_g. The leakage current path is equivalent to an LC resonant circuit in series with the CM voltage [11], and the CM voltage v_{CM} is defined as

$$v_{\mathrm{CM}} = \frac{v_{\mathrm{AN}} + v_{\mathrm{BN}}}{2} + (v_{\mathrm{AN}} - v_{\mathrm{BN}})\frac{L_2 - L_1}{2(L_1 + L_2)} \tag{1}$$

Where v_{AN} is the voltage difference between points A and N,v_{BN} is the voltage difference between points B and N. L_1 and$L_2$are the output filter inductors.

$$v_{\mathrm{CM}} = \frac{v_{\mathrm{AN}} + v_{\mathrm{BN}}}{2} - \frac{(v_{\mathrm{AN}} - v_{\mathrm{BN}})}{2} = v_{\mathrm{BN}} \tag{2}$$

The full-bridge inverters only need half of the input voltage value demanded by the half-bridge topology, and the filter inductors$L_1$and$L_2$are usually with the same value. As a result,(1) is simplified as

$$v_{\mathrm{CM}} = \frac{v_{\mathrm{AN}} + v_{\mathrm{BN}}}{2} \tag{3}$$

Fig.3 (a) shows the H5 topology. It employs an extra switch on the dc side of inverter. As a result, the PV array is disconnected from the utility grid when the inverter output voltage is at zero voltage level, and the leakage current path is cut off. The HERIC topology shown in Fig.3 (b) employs two extra switches on the ac side of inverter, so the leakage current path is cut off as well. However, its power device cost is higher than that of the H5 topology. Fig.3 (c) and (d) shows the H6-type topology and the hybrid-bridge topology respectively. Comparing with a full-bridge inverter, two extra switches are employed in the dc sides of these two topologies. Further more, both the H5 topology and the HERIC topology have been compared in terms of efficiency and leakage currents characteristics [12]. However,these topologies have never been analyzed form the point of view of topological relationships.

In this paper, a family of novel H6 full-bridge topologies is proposed for the transformerless PV induction motor tied inverter. An extraswitch is inserted to the H5 topology for forming a new current path and for the purpose of reducing conduction loss. Therefore,in the active modes, the inductor current of the proposed H6topology flows through two switches during one of the halfline periods and through three switches during another half-line period. As a result, for comparing with the topologies presented in [13], [14], and [15], the proposed H6 topology has achieved the minimum conduction loss, and also has featured with low leakage currents. On the other hand, the topological relationship between H5 topology and HERIC topology is revealed, and the methods for generating HERIC topology from H6-type topology and from hybrid-bridge topology are presented, respectively.

This paper is organized as follows. In the operation modes and characteristics of the H5 topology and the HERIC topology are presented and compared. The methods ofgenerating HERIC topology from the H6-type topology or from the hybrid-bridge topology are given. A family of H6 topologies is proposed, and the topological relationship between H5 topology and HERIC topology is analyzed. In one of the proposed H6 topologies is taken as an example for analysis in detail with operational principle and modulation strategy.The comparisons between H5, HERIC, and the proposed H6topology are given in terms of power loss and device cost.

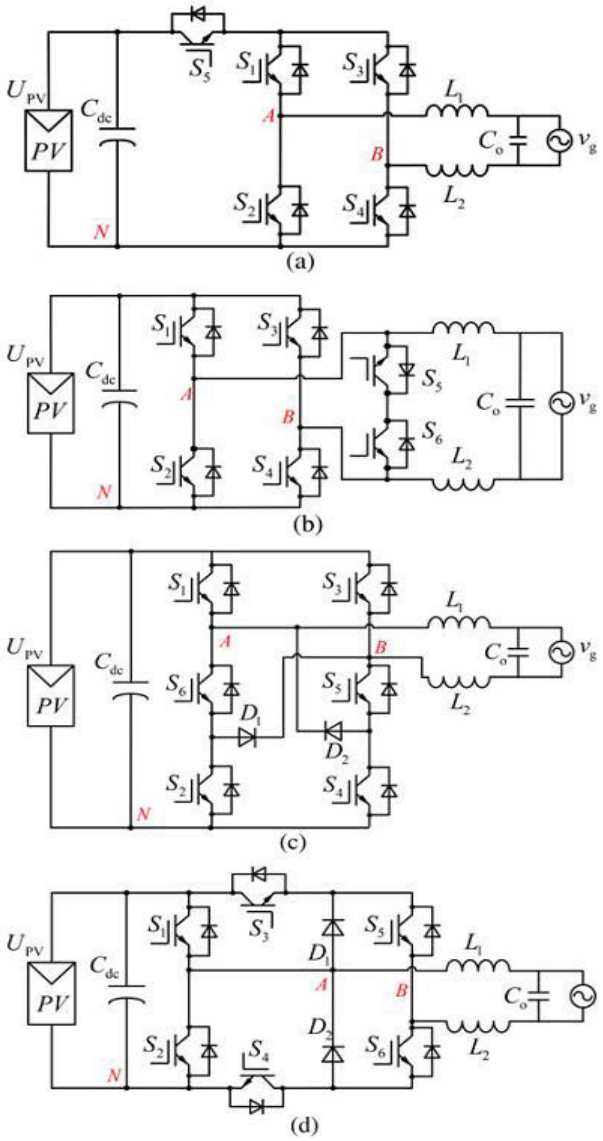

Fig.3. Four typical topologies of transformerless full-bridge inverters. (a). H5. (b) HEIRC. (c) H6-type. (d) Hybrid bridge.

II. COMPARATIVE ANALYSIS ON EXISTING TOPOLOGIES

A. Operation Modes of H5 and HERIC

The operation modes of H5 topology and HERIC topologyare taken as examples for analysis. There are four operation modes in each period of the utility grid of the H5 topology, as shown in Fig.4. It can be seen that in the active modes, the inductor current of H5 topology is always flowing through three switches due to its extra switch S5 in dc side. In the freewheeling modes, the inductor current of H5 topology is flowing through two switches.

There are four operation modes in each period of the utilitygrid of the HEIRC topology, as shown in Fig.5. It can be seen that the inductor current of HERIC topology is always flowing through two switches in the active modes. In the freewheeling modes, the inductor current of HERIC topology is flowing through two switches.

Therefore, although the H5 topology features less power devices than the HERIC topology, its conduction loss is higher than that of the HERIC topology. Moreover, the conductionlosses of the H6-type topology and the hybrid-bridge topologyare also higher than that of the HERIC topology due to extra switches in the dc side. As a result, the conduction losses of H5topology, H6 topology, and hybrid-bridge topology should be reduced for the harvest of higher efficiency.

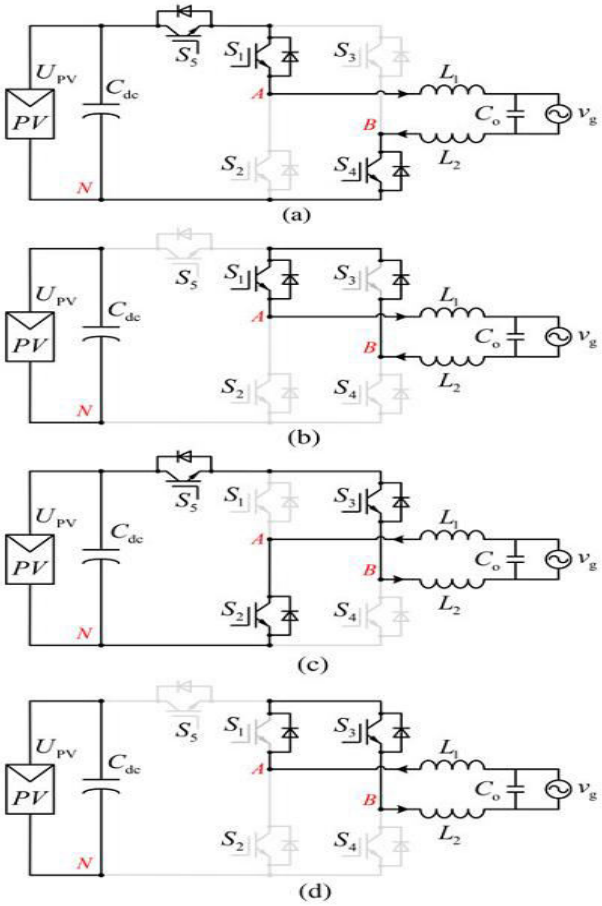

Fig.4. Operation modes of H5 topology. (a) Active mode in the positive half period. (b) Freewheeling mode in the positive half period. (c) Active mode in the negative half period. (d) Freewheeling mode in the negative half period.

B. Topology Relationship

The H6-type topology is taken as an example to analysis first. From Fig.3 (c), it can be seen that there are two switches between the terminal(A) and the negative terminal of the PVarray, and there are another two switches between the terminal(B) and the negative terminal of the PV array. Therefore, the inductor current is controlled to flow through three switches in the active modes of H6-type topology. In order to reduce the conduction loss, the collector of switch$S_2$is disconnected from the anode of diodeD_1, and then it is connected to the

terminal (A), as shown in Fig.6 (a). As a result, the inductor current flows through S_2 and S_3 instead of S_2, S_3, and S_6 in the active mode during the negative half cycle of the grid voltage. The dc and ac sides of this topology are still disconnected in the free wheeling modes. The same means are applied to another leg, where the switch S_4 is disconnected from the diode D_2 and then connected to the terminal (B), as shown in Fig.6 (b).

Hence, a circuit structure of HERIC topology is derived by the methods described in Fig.6. The topology is shown in Fig.7.Compared with the HERIC topology shown in Fig.3 (c), the form of the bidirectional switch in ac side is changed.

Similarly, another circuit structure of HERIC topology can be derived from the hybrid-bridge shown in Fig.3 (d). The switches S_3 and S_4 are disconnected from D_1 and D_2, respectively, and then connect both of them to the terminal (B), as shown in Fig.8. However, there is only one extra switch in dc side of the H5 topology. When the emitter of S_5 is disconnected from S_1 and connected to the terminal (A), the inductor current flows through S_4 and S_5 instead of S_1, S_4, and S_5 in the active mode of positive half cycle of the grid voltage. Hence, the conduction loss is reduced. Unfortunately, in the active mode of negative half cycle of the grid voltage, there is no inductor current path, as shown in Fig.9 (a). Therefore, an extra switch S6 is introduced into the topology between the positive terminal of the PV array and the terminal (B) to form a new current path. As a result, the circuit structure of the HERIC topology shown in Fig.3 (b) is derived from the H5 topology, as shown in Fig.9 (b).

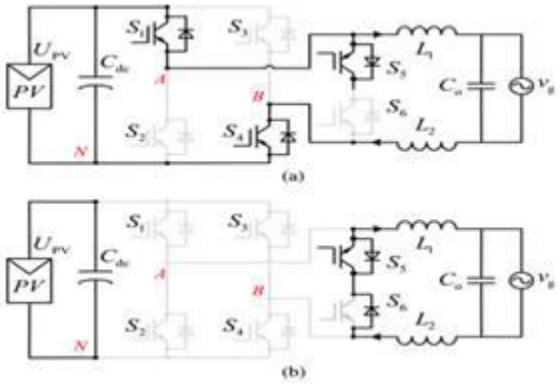

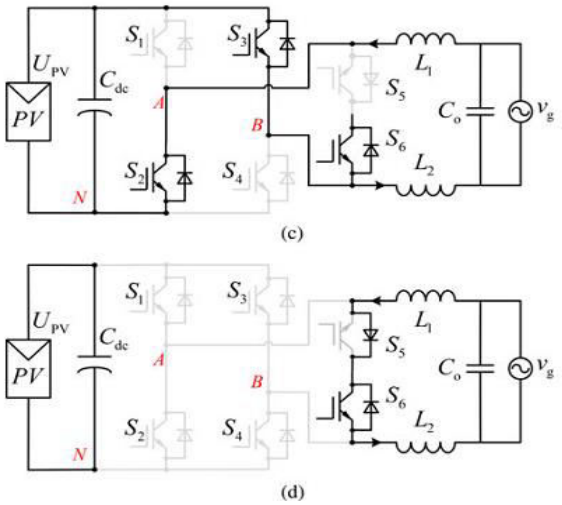

Fig.5Operation modes of HERIC topology. (a) Active mode in the positivehalf period. (b) Freewheeling mode in the positive half period. (c) Active modein the negative half period. (d) Freewheeling mode in the negative half period.

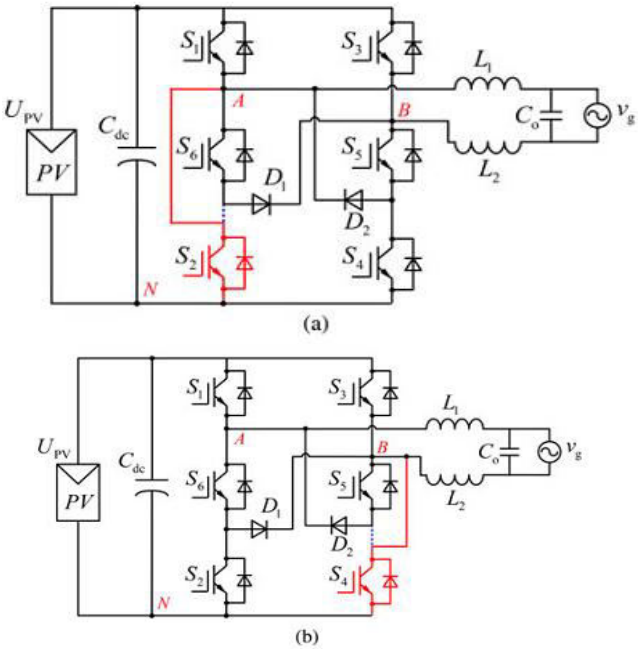

Fig.6. Modified H6-type inverter topologies. (a) Circuit structure A. (b) Circuit structure B

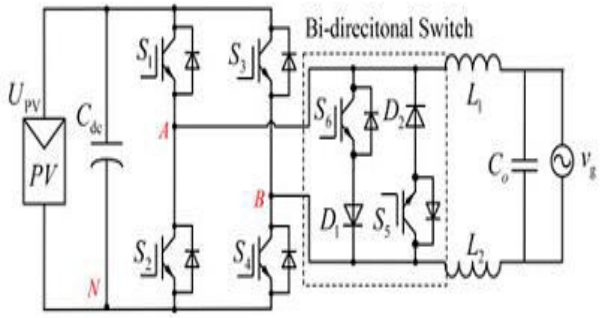

Fig.7. Another circuit structure of HERIC topology.

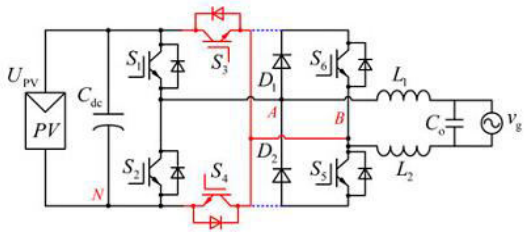

Fig.8. Another circuit structure of HERIC topology derived from hybridbridge topology.

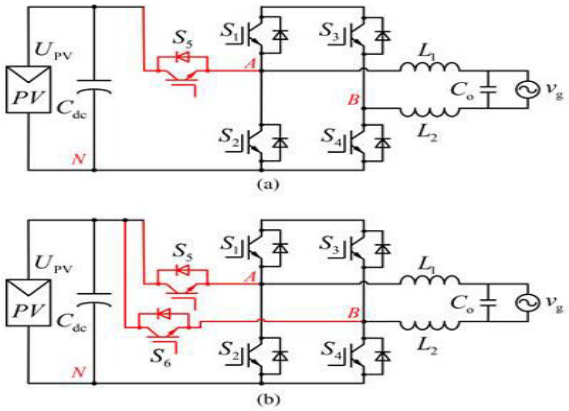

Fig.9. Relationship between HERIC topology and H5 topology. (a) ModifiedH5 topology. (b) HERIC topology derived from H5 topology.

Therefore, we can derive various HERIC topologies based onthe existing topologies, such as the H6-type topology, hybrid bridge topology and H5 topology, for the purpose of reducing conduction loss.

III. ANALYSIS ON THE H6 TOPOLOGY AND COMPARISON WITH OTHER TOPOLOGIES

A. Novel H6 Topology

From the mentioned analysis, an extra switchS_6 is introduced into the H5 inverter topology between the positive terminal of the PV array and the terminal (B) to form a new current path. As a result, a novel H6 transformerless full-bridge inverter topology is derived, as shown in Fig.10 (a).

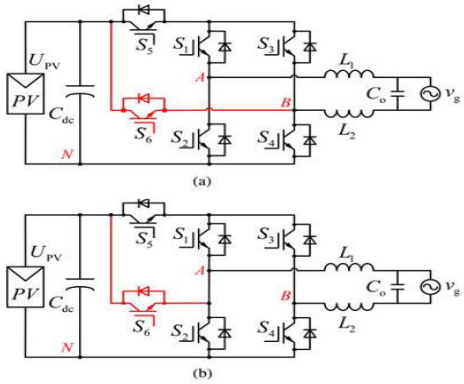

Fig.10. A family of proposed H6-type inverter topologies. (a). Circuit structureA. (b) Circuit structure B.

Similarly, the extra switchS_6 can be introduced into the H5 inverter topology between the positive terminal of the PV array and the terminal (A) to form a new current path as well, as shown in Fig.10 (b). Therefore, a new circuit structure of novel H6 inverter is presented. As a result, the conduction loss of the proposed H6 topologies is higher than HERIC topology and lessthan H5 topology.

B. Operation Mode Analysis

The circuit structure of proposed novel H6 inverter topologies shown in Fig.10 (a) is taken as an example to analysis. PV grid-tied systems usually operate with unity power factor. Thewaveforms of the gate drive signals for the proposed novel H6 topology are shown in Fig.11, where vg is the voltage of utility grid.i_{ref} is the inductor current reference.$v_{gs1}$to vgs6 represent the gate drive signals of switchesS_1toS_6, respectively.

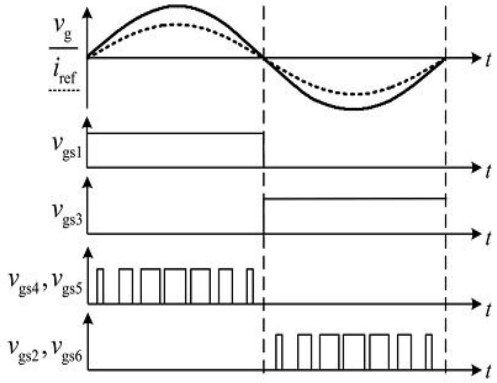

Fig.11. Schematic of gate drive signals with unity power factor.

There are four operation modes in each period of the utilitygrid, as shown in Fig.12, where v_{AN} represents the voltage between terminal (A) and terminal (N) and v_{BN} represents the voltage between terminal (B) and terminal (N).$v_{AB}$is the DM voltage of the topology,$v_{AB}=v_{AN}-v_{BN}$. The CM voltage $v_{CM}=0.5(v_{AN}+v_{BN})$.

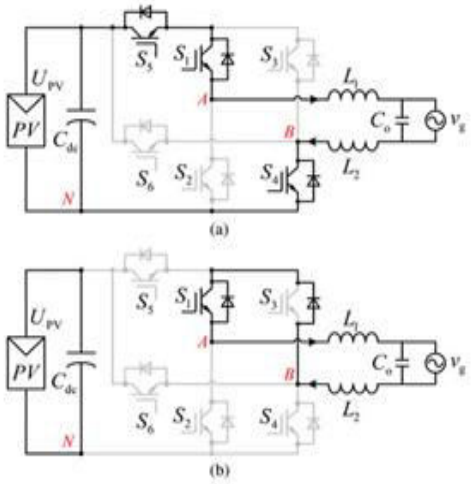

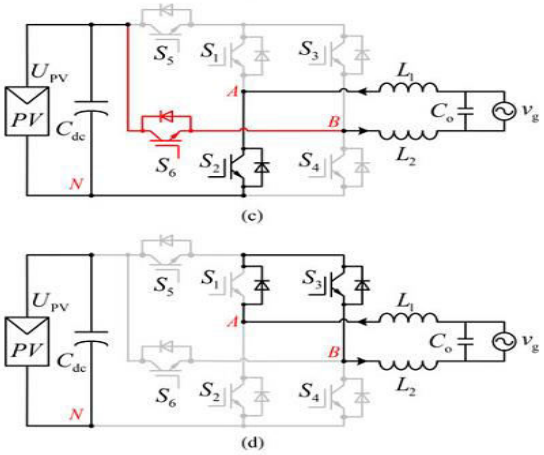

Fig.12. Equivalent circuits of operation modes. (a) Active mode in the positive half period. (b) Freewheeling mode in the positive half period. (c) Active mode in the negative half period. (d) Freewheeling mode in the negative half period.

a) Mode I is the active mode in the positive half period ofthe utility grid voltage, as shown in Fig.12 (a). S_1,S_4,andS_5 are turned ON, and the other switches are turnedOFF. The inductor current is flowing throughS_1,S_4, andS_5.v_{AN}=U_{PV},v_{BN}=0; thus,v_{AB}=U_{PV}, and the CM voltage CM=(v_{AN}+v_{BN})/2=0.5U_{PV}.

b) Mode II is the freewheeling mode in the positive half period of the utility grid voltage, as shown in Fig.12 (b).$S_1$is turned ON; the other switches are turned OFF. The inductor current is flowing through $S_1$and the anti parallel diode ofS3. v_{AN}=v_{BN}≈0.5U_{PV}; thus, v_{AB}=0, and the CM voltagev_{CM}=(v_{AN}+v_{BN})/2≈0.5U_{PV}.

c) Mode III is the active mode in the negative half period ofthe utility grid voltage, as shown in Fig.12 (c).S_2,S_3, andS_6 are turned ON; the other switches are turned OFF. The inductor current is flowing through S_2 andS_6. Although $S_3$is turned ON, there is no current flowing through it, and the switch S_3 has no conduction loss in this mode. Never the less, in the H5 topology, the inductor current flows through S_2,S_3, and S_5. Therefore, the conduction loss of proposed topology is less than that of H5 topology. In this mode,v_{AN}=0,v_{BN}=U_{PV}; thus,v_{AB}=−, and the CM voltagev_{CM}=(v_{AN}+v_{BN})/2=0.5U_{PV}.

d) Mode IV is the freewheeling mode in the negative half period of the utility grid voltage, as shown in Fig.12 (d).$S_3$is turned ON, and the other switches are turned OFF. The inductor current is flowing through S_3 and the antiparallel diode of S_1. v_{AN}=v_{BN}≈0.5U_{PV}; thus,v_{AB}=0,and the CM voltagev_{CM}=(v_{AN}+v_{BN})/2≈0.5U_{PV}.

IV. INDUCTION MOTOR

An asynchronous motor type of an induction motor is an AC electric motor in which the electric current in the rotor needed to produce torque is obtained by electromagnetic induction from the magnetic field of the stator winding. An induction motor can therefore be made without electrical connections to the rotor as are found in universal, DC and synchronous motors. An asynchronous motor's rotor can be either wound type or squirrel-cage type.

Three-phase squirrel-cage asynchronous motors are widely used in industrial drives because they are rugged, reliable and economical. Single-phase induction motors are used extensively for smaller loads, such as household appliances like fans. Although traditionally used in fixed-speed service, induction motors are increasingly being used with variable-frequency drives (VFDs) in variable-speed service. VFDs offer especially important energy savings opportunities for existing and prospective induction motors in variable-torque centrifugal fan, pump and compressor load applications. Squirrel cage induction motors are very widely used in both fixed-speed and variable-frequency drive (VFD) applications. Variable voltage and variable frequency drives are also used in variable-speed service.

In both induction and synchronous motors, the AC power supplied to the motor's stator creates a magnetic field that rotates in time with the AC oscillations. Whereas a synchronous motor's rotor turns at the same rate as the stator field, an induction motor's rotor rotates at a slower speed than the stator field. The induction motor stator's magnetic field is therefore changing or rotating relative to the rotor. This induces an opposing current in the induction motor's rotor, in effect the motor's secondary winding, when the latter is short-circuited or closed through external impedance. The rotating magnetic flux induces currents in the windings of the rotor; in a manner similar to currents induced in a transformer's secondary winding(s). The currents in the rotor windings in turn create magnetic fields in the rotor that react against the stator field. Due to Lenz's Law, the direction of the magnetic field created will be such as to oppose the change in current through the rotor windings. The cause of induced current in the rotor windings is the rotating stator magnetic field, so to oppose the change in rotor-winding currents the rotor will start to rotate in the direction of the rotating stator magnetic field. The rotor accelerates until the magnitude of induced rotor current and torque balances the applied load. Since rotation at synchronous speed would result in no induced rotor current, an induction motor always operates slower than synchronous speed.The difference, or "slip," between actual and synchronous speed varies from about 0.5 to 5.0% for standard Design B torque curve induction motors. The induction machine's essential character is that it is created solely by induction instead of being separately excited as in synchronous or DC machines or being self-magnetized as in permanent magnet motors.

For rotor currents to be induced the speed of the physical rotor must be lower than that of the stator's rotating magnetic field ($\boldsymbol{n_s}$); otherwise the magnetic field would not be moving relative to the rotor conductors and no

currents would be induced. As the speed of the rotor drops below synchronous speed, the rotation rate of the magnetic field in the rotor increases, inducing more current in the windings and creating more torque. The ratio between the rotation rate of the magnetic field induced in the rotor and the rotation rate of the stator's rotating field is called slip. Under load, the speed drops and the slip increases enough to create sufficient torque to turn the load. For this reason, induction motors are sometimes referred to as asynchronous motors. An induction motor can be used as an induction generator, or it can be unrolled to form a linear induction motor which can directly generate linear motion.

Synchronous Speed:

The rotational speed of the rotating magnetic field is called as synchronous speed.

$$Ns = \frac{120 \times f}{P} \quad (RPM) \tag{4}$$

Where, f = frequency of the supply

P = number of poles

Slip:

Rotor tries to catch up the synchronous speed of the stator field, and hence it rotates. But in practice, rotor never succeeds in catching up. If rotor catches up the stator speed, there won't be any relative speed between the stator flux and the rotor, hence no induced rotor current and no torque production to maintain the rotation. However, this won't stop the motor, the rotor will slow down due to lost of torque, the torque will again be exerted due to relative speed. That is why the rotor rotates at speed which is always less the synchronous speed.

The difference between the synchronous speed (Ns) and actual speed (N) of the rotor is called as slip.

$$\% \text{ slip} \quad s = \frac{Ns - N}{Ns} \times 100 \tag{5}$$

V. MATLAB/SIMULINK RESULTS

Case I: CM voltage and leakage current in H5 topology

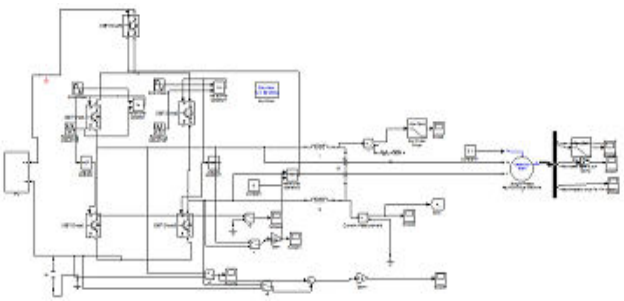

Fig.13 Simulink model of H5 Topology

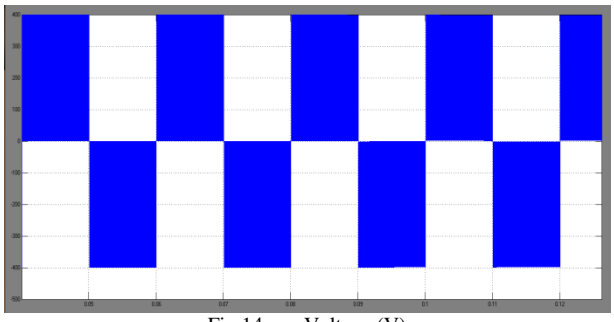

Fig.14 v_{AN} Voltage (V)

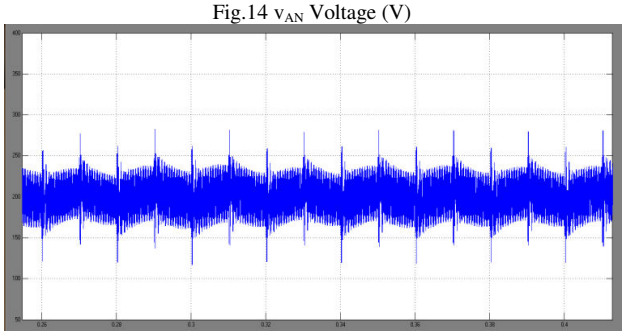

Fig.15V_{BN} Voltage (V)

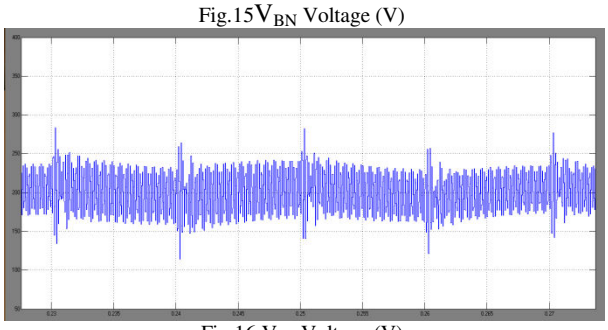

Fig.16 V_{CN} Voltage (V)

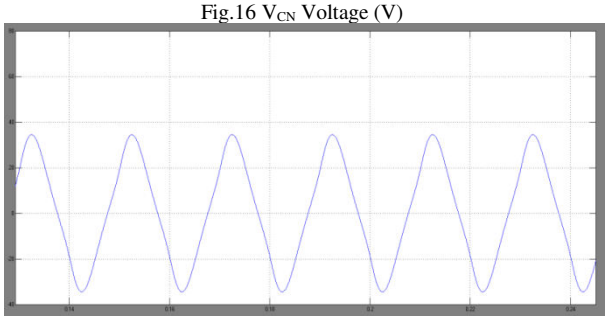

Fig.17Ig Current

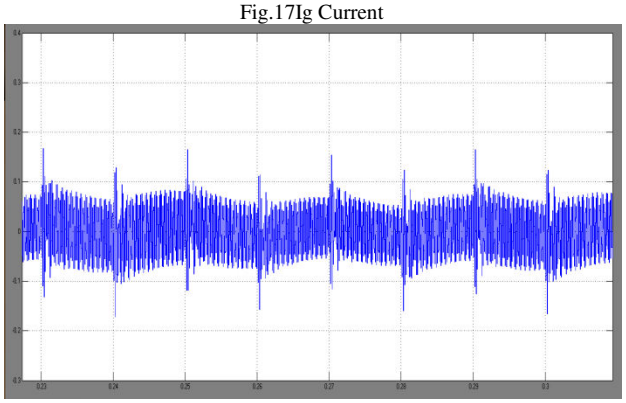

Fig.18 Leakage Current

Case II: CM voltage and leakage current in H5 topology with Induction motor

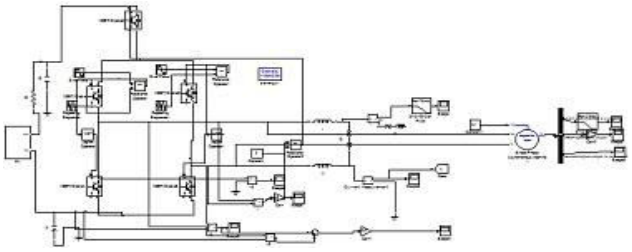

Fig.19 Simulink model of H5 Topology with IM

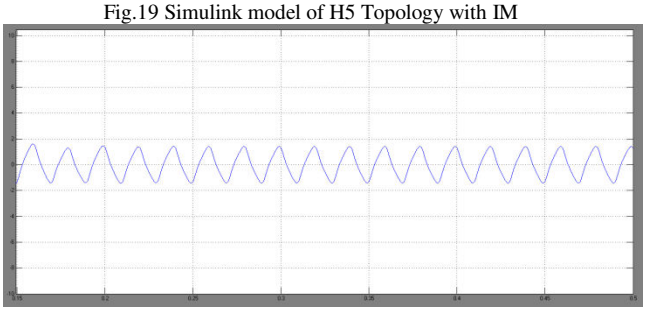

Fig.20 Motor Current

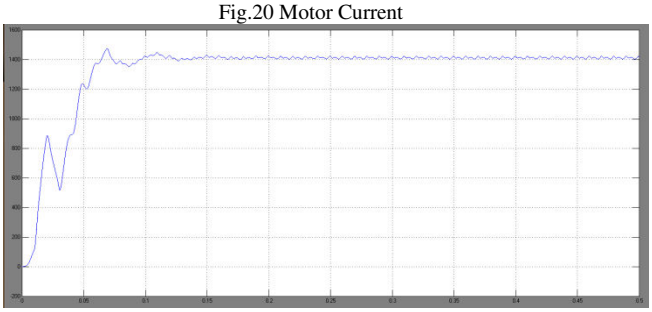

Fig.21 Speed Characteristics of the motor

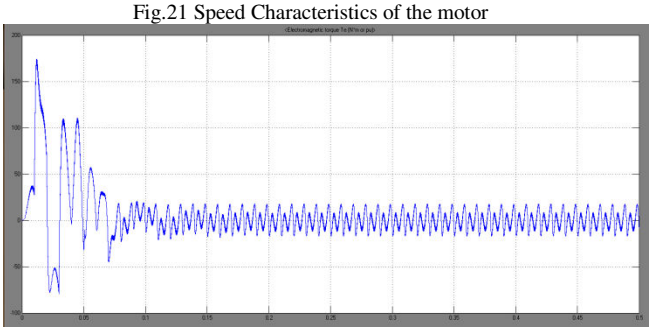

Fig.22 Torque Characteristics of the motor

Case III: CM voltage and leakage current in H6 topology

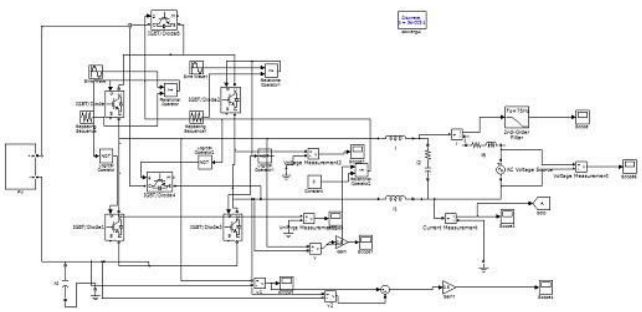

Fig.23 Simulink model of H6 Topology

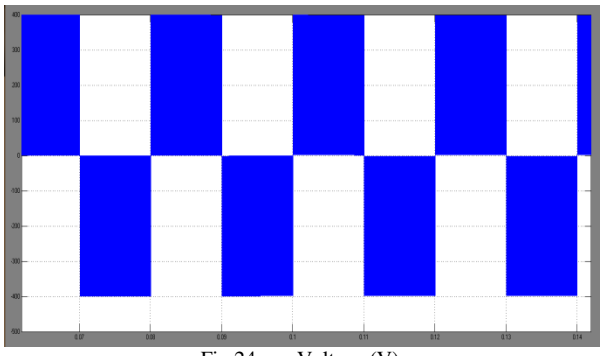

Fig.24 v_{AN} Voltage (V)

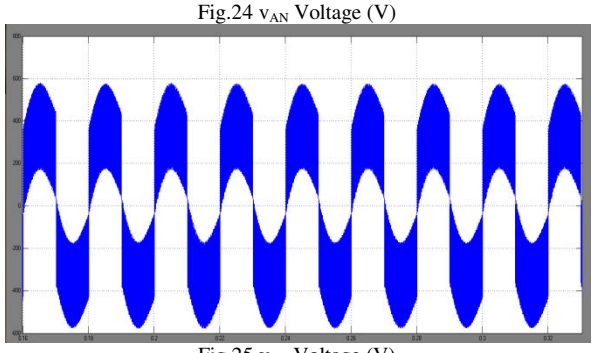

Fig.25 v_{BN} Voltage (V)

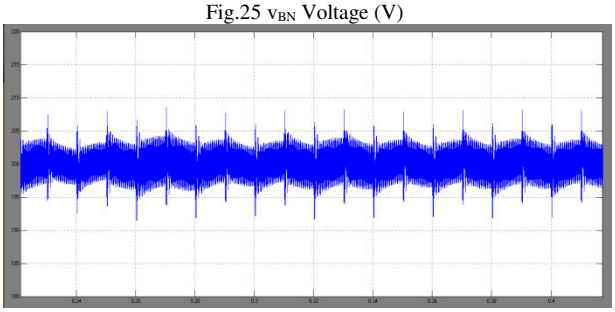

Fig.26v_{CN} Voltage (V)

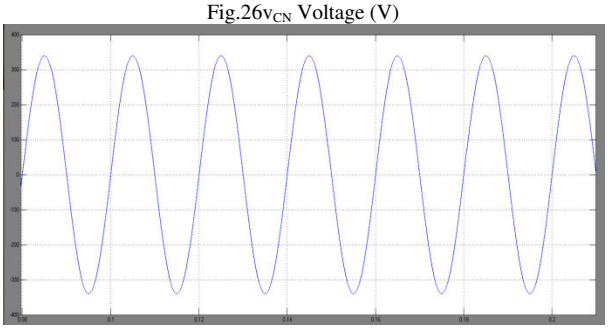

Fig.27 OutputVoltage (V)

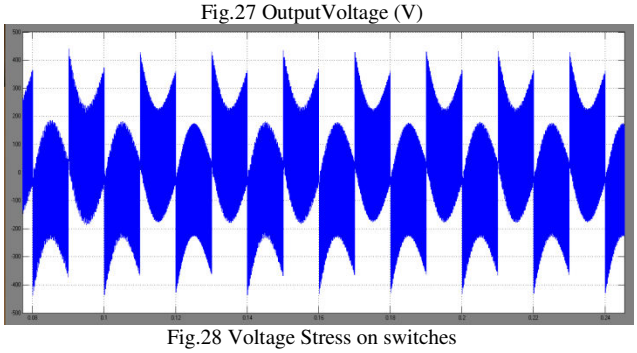

Fig.28 Voltage Stress on switches

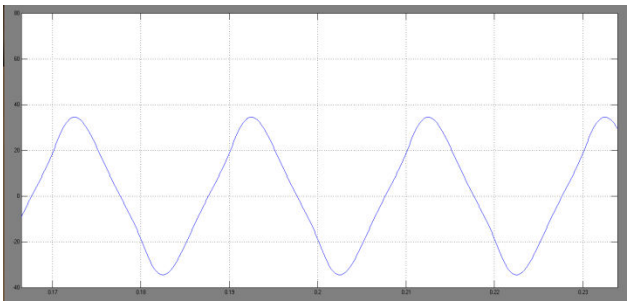

Fig.29 Ig Current

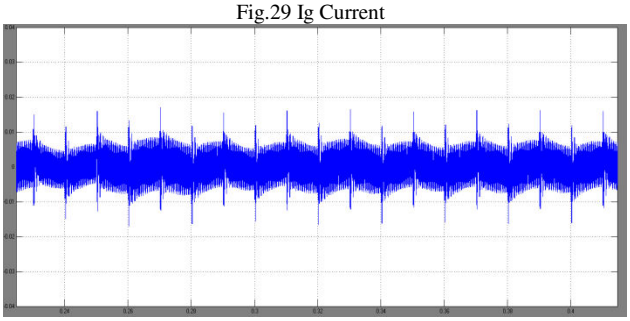

Fig.29 Leakage Current

Case IV: CM voltage and leakage current in H6 topology With Induction motor

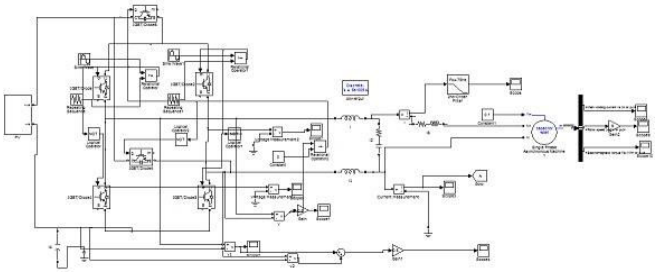

Fig.30 Simulink model of H6 topology With Induction motor

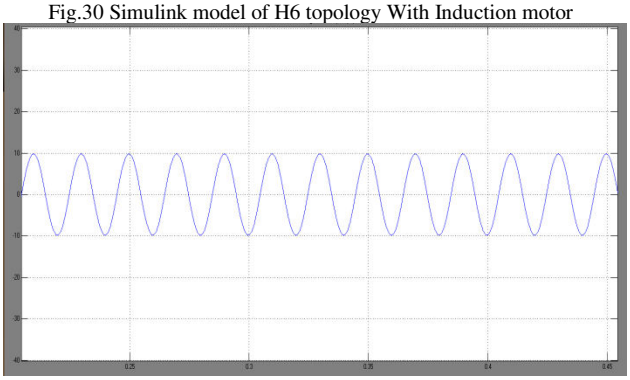

Fig.31 Armature Current

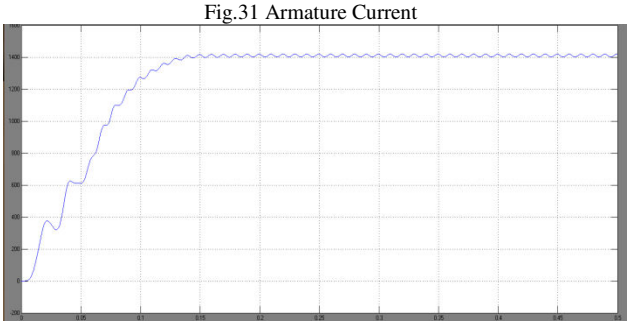

Fug.32 Speed Characteristics of the motor

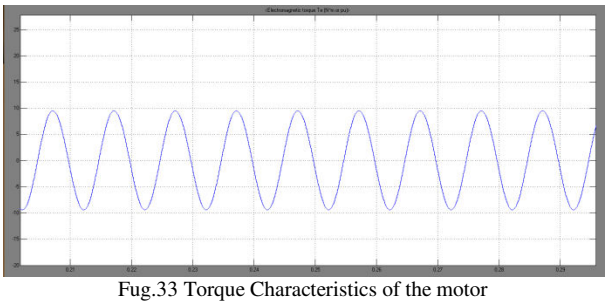

Fug.33 Torque Characteristics of the motor

Case V: CM voltage and leakage current in HERIC topology

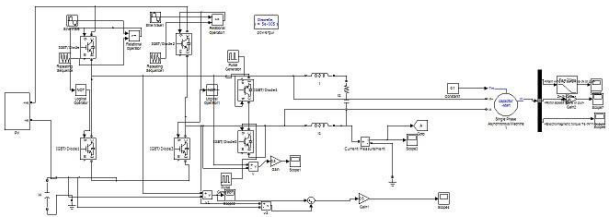

Fig.34 Simulink model of HERIC Topology

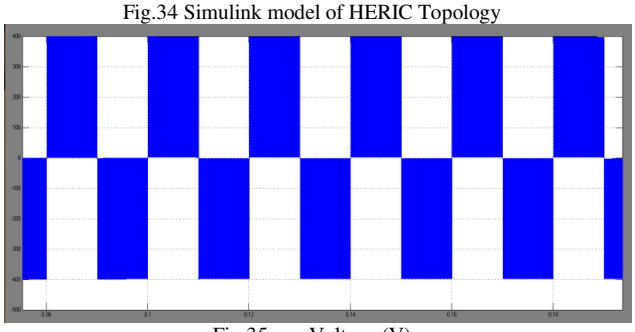

Fig.35 v_{AN} Voltage (V)

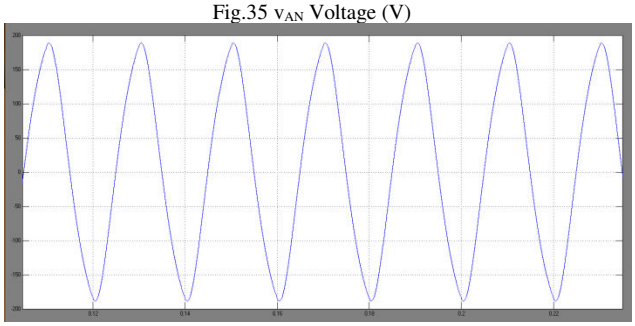

Fig.36 Switch Voltage (V)

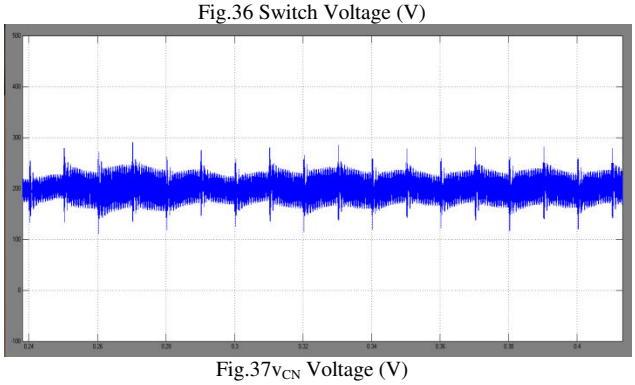

Fig.37v_{CN} Voltage (V)

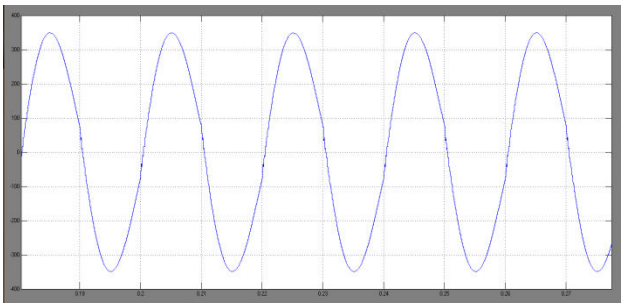

Fig.38 Output Voltage (V)

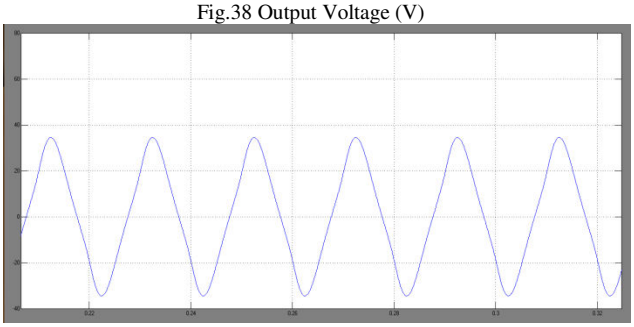

Fig.39 Ig Current

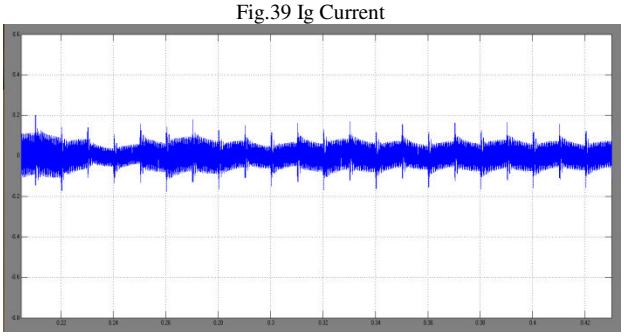

Fig.40Leakage Current

Case VI: CM voltage and leakage current in HERIC topology with Induction motor

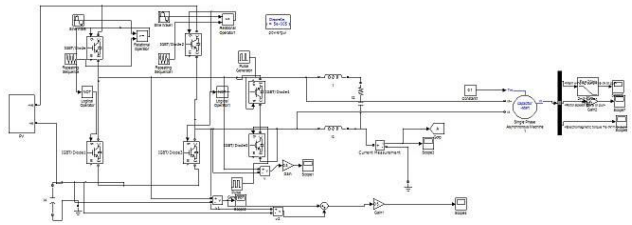

Fig.41 Simulink model of HERIC Topologywith Induction motor

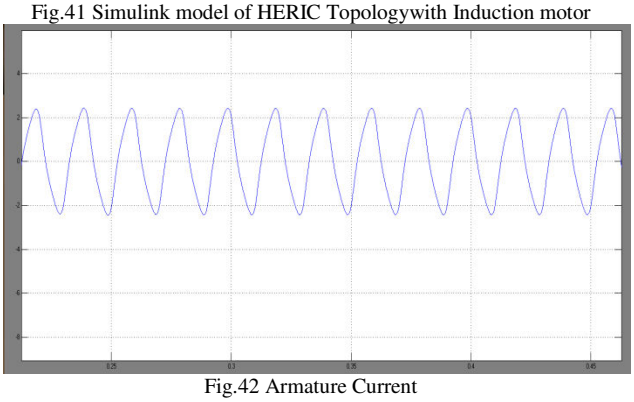

Fig.42 Armature Current

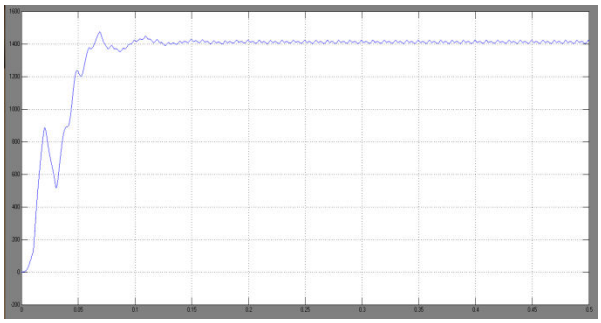

Fig.43 Speed Characteristics of the motor

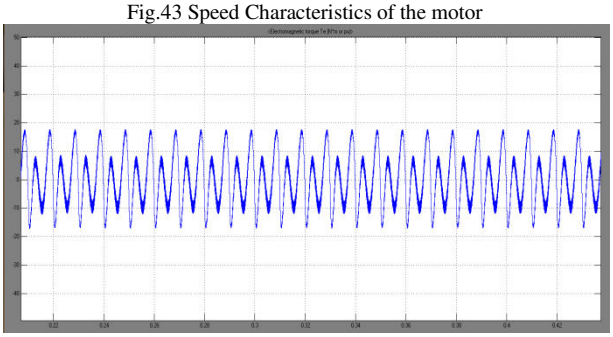

Fig.44 Torque Characteristics of the motor

VI. CONCLUSION

Transformerless PV inverter has many advantages, for instance: cost, size, and weight reduction. In addition, it increases the whole system efficiency, certainly depending on the topology a leakage current should appear. Recently, many topologies of transformerless PV inverters have been proposed, trying to reduce the leakage current at the ground connection. Following this trend, this paper proposes a new transformerless inverter for PV generation systems.As compared to the other inverters i.e., H5 and HERIC bridge topologies the H6 topology is more efficient .This inverter provided to induction motor with smooth output, better voltage and the switching loss reduce in this topology.

REFERENCES

[1] S. B. Kjaer, J. K. Pederson, and F. Blaabjerg, "A review of single-phasegrid-connected inverters for photovoltaic modules,"IEEE Trans. Ind.Appl., vol. 41, no. 5, pp. 1292–1306, Sep/Oct. 2005.

[2] F. Blaabjerg, Z. Chen, and S. B. Kjaer, "Power electronics as efficientinterface in dispersed power generation systems," IEEE Trans. PowerElectron., vol. 19, no. 5, pp. 1184–1194, Sep. 2004.

[3] B. Sahan, A. N. Vergara, N. Henze, A. Engler, and P. Zacharias, "A singlestage PV module integrated converter based on a low-power current sourceinverter," IEEE Trans. Ind. Electron., vol. 55, no. 7, pp. 2602–2609, Jul.2008.

[4] M. Calais, J. Myrzik, T. Spooner, and V. G. Agelidis, "Inverters for singlephase grid connected photovoltaic systems—An overview," inProc. IEEEPESC, 2002, vol. 2, pp. 1995–2000.

[5] F. Blaabjerg, Z. Chen, and S. B. Kjaer, "Power electronics as efficientinterface in dispersed power generation systems," IEEE Trans. PowerElectron., vol. 19, no. 5, pp. 1184–1194, Sep. 2004.

[6] Q. Li and P. Wolfs, "A review of the single phase photovoltaic moduleintegrated converter topologies with three different dc link

configuration," IEEE Trans. Power Electron., vol. 23, no. 3, pp. 1320–1333, May2008.
[7] O. Lopez, F. D. Freijedo, A. G. Yepes, P. Fernandez-Comesana, J. Malvar,R. Teodorescu, and J. Doval-Gandoy, "Eliminating ground current in atransformerless photovoltaic application,"IEEE Trans. Energy Convers.,
vol. 25, no. 1, pp. 140–147, Mar. 2010.
[8] R. Gonzalez, J. Lopez, P. Sanchis, and L. Marroyo, "Transformerlessinverter for single-phase photovoltaic systems,"IEEE Trans. Power Electron., vol. 22, no. 2, pp. 693–697, Mar. 2007.[9] H. Xiao and S. Xie, "Leakage current analytical model and application in single-phase transformerless photovoltaic grid-connected inverter,"IEEE Trans. Electromagn. Compat., vol. 52, no. 4, pp. 902–913, Nov.2010.
[10] VDE-AR-N 4105: Power Generation Systems Connected to the LowVoltage Distribution Network—Technical Minimum Requirements For theConnection to and Parallel Operation with Low-Voltage Distribution Networks, DIN_VDE Normo, 2011–08.
[11] B. Yang, W. Li, Y. Gu, W. Cui, and X. He, "Improved transformerlessinverter with common-mode leakage current elimination for a photovoltaicgrid-connected power system,"IEEE Trans. Power Electron., vol. 27,no. 2, pp. 752–762, Feb. 2012.
[12] R. Gonzalez, E. Gubia, J. Lopez, and L. Marroyo, "Transformerless singlephase multilevel-based photovoltaic inverter,"IEEE Trans. Ind. Electron.,vol. 55, no. 7, pp. 2694–2702, Jul. 2008.
[13] H. Xiao and S. Xie, "Transformerless split-inductor neutral point clampedthree-level PV grid-connected inverter," IEEE Trans. Power Electron.,vol. 27, no. 4, pp. 1799–1808, Apr. 2012.
[14] L. Zhang, K. Sun, L. Feng, H. Wu, and Y. Xing, "A family of neutral pointclamped full-bridge topologies for transformerless photovoltaic grid-tiedinverters,"IEEE Trans. Power Electron., vol. 28, no. 2, pp. 730–739, Feb.2012.
[15] German Patent Wechselrichter: DE 19642522C1 Apr. 1998.